DOI: 10.14744/eer.2024.95530
Eur Eye Res 2024;4(3):209–216

EUROPEAN EYE RESEARCH

ORIGINAL ARTICLE

Quantitative assessment of the parafoveal vessel density and ganglion cell inner plexiform layer thickness in non-proliferative macular telangiectasia type 2

Aylin Karalezli,[1] Cansu Kaya,[1] Sema Kaderli,[2] Ahmet Kaderli,[1] Sabahattin Sul[1]

[1]Department of Ophthalmology, Mugla Sitki Kocman University, Mugla, Türkiye
[2]Department of Ophthalmology, Mugla Training and Research Hospital, Mugla, Türkiye

Abstract

Purpose: The study aimed to evaluate the vessel densities (VDs) and ganglion cell inner plexiform layer (GCIPL) thicknesses in macular telangiectasia (MacTel) Type 2.

Methods: Thirty-six eyes with MacTel Type 2 and 30 controls were included in this prospective study. Based on the presence of ellipsoid zone (EZ) disruption two groups were formed: Group 1, MacTel eyes with intact EZ. Group 2; with EZ disruption.

Results: In all MacTel eyes, a decrease was obtained in VDs and temporal parafoveal thickness in 1st year. (For group 1 p=0.006, p=0.045. For group 2 p=0.002, p=0.02) The average and minimum GCIPL also decreased in Group 2. (For average p=0.005, for minimum p=0.003) The mean VD, temporal and nasal thicknesses, average minimum GCIPL, and retinal nerve fiber layer were lower in Group 2 in the final visit.

Conclusion: VDs and GCIPL thickness may be useful parameters in the follow-up of MacTel Type 2 disease in which microvascular changes are observed in parallel with neurodegeneration.

Keywords: Ganglion cell inner plexiform layer thickness, nonproliferative macular telangiectasia, parafoveal vessel density

Macular telangiectasia (MacTel) Type 2 is an idiopathic bilateral disease with capillary structural alterations and degeneration of the outer retina in the fovea or perifoveal region.[1] Gass and Blodi in 1993 provided a five-stage classification of MacTel Type 2, later Yannuzzi et al., simplified the classification into two stages: non-proliferative and proliferative.[2,3]

Characteristic structural alterations of MacTel Type 2 are dilated and right-angled vessel and telangiectatic capillaries decreased retinal transparency, and retinal pigment clumps on fundus photography.[4,5] The morphological changes observable in optical coherence tomography (OCT) images are thinning of the central retina, hyporeflective spaces in the inner and outer retina,

Cite this article as: Karalezli A, Kaya C, Kaderli S, Kaderli A, Sul S. Quantitative assessment of the parafoveal vessel density and ganglion cell inner plexiform layer thickness in non-proliferative macular telangiectasia type 2. Eur Eye Res 2024;4(3):209–216.

Correspondence: Sema Kaderli, M.D. Department of Ophthalmology, Mugla Training and Research Hospital, Mugla, Türkiye
E-mail: sematamerkaderli@hotmail.com
Submitted Date: 02.04.2024 **Revised Date:** 13.05.2024 **Accepted Date:** 25.06.2024 **Available Online Date:** 29.11.2024

and focal disruption of the ellipsoid zone (EZ) that typically starts temporal to the foveal center, then progressively involves the center and nasal macula.[6] Previous studies have demonstrated an increase in EZ loss and a correlated reduction in retinal sensitivity in eyes with MacTel as the disease progresses.[7-9]

In this study, our aim is to compare the quantitative OCT angiography (OCTA) parameters according to EZ integrity in eyes with MacTel type 2 in the non-proliferative stage with controls. We also aim to investigate the changes between the baseline and 1 year later values in MacTel patients.

Materials and Methods

The 36 eyes with MacTel Type 2 have been included in this prospective study. This current study was accepted by the Local Institutional Ethics Committee by all ethical standards stated in the Declaration of Helsinki. (Approval number: 18/IV, date: August 26, 2021) The individuals got knowledge about the study and the disease to be administered, and the written informed consent form was acquired.

Inclusion criteria were diagnosis of non-proliferative MacTel Type 2 disease followed at least 1 year. Patients with any history of glaucoma, uveitis or other retinal diseases, retinal vascular diseases, choroidal neovascularization, an intravitreal treatment, or ocular surgery history were excluded from the study.

MacTel was diagnosed due to clinical properties in the parafovea such as retinal crystalline deposits, right-angled venules, telangiectatic vessels, pigment clusters, and decrease of retinal transparency as described by gass and approved by failure frequency analysis (FFA) and OCT (hyporeflective inner retinal cavities, internal limiting membrane [ILM] drape, outward bending of inner retinal layers, EZ disruption). OCTA (RTVue; Optovue, CA) was performed in whole participants. Thirty healthy age-matched eyes were enrolled in this study as a control group. In our study, we divided our non-proliferative MacTel Type 2 cases into two groups with respect to the presence of EZ disruption: Group 1: MacTel Type 2 eyes with intact EZ, Group 2: MacTel Type 2 eyes with EZ disruption (Fig. 1).

Baseline clinical information and follow-up notes of all participants were evaluated and saved. An ophthalmic examination including best-corrected visual acuity (BCVA) (logMAR), slit-lamp, and fundus examination was performed on all participants. FFA performed with Zeiss (Visucam 500, Dublin, USA).

OCT (Spectralis OCT, Heidelberg, Germany) analysis included

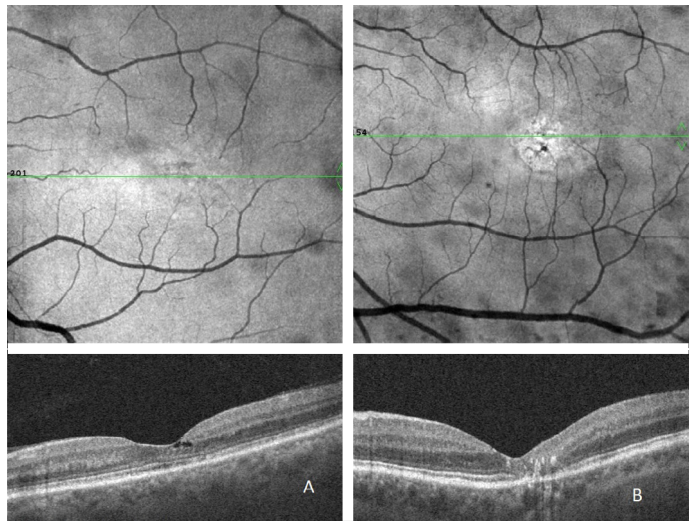

Fig. 1. Non-proliferative macular telangiectasia (MacTel) type 2 cases divided into two groups according to the presence of ellipsoid zone disruption. **(a)** The enface and B-scan image of a MacTel type 2 eye with intact ellipsoid zone. **(b)** The enface and B-scan image of MacTel type 2 eye with ellipsoid zone disruption.

central macular thickness (CMT) (μm) defined from the ILM to retinal pigment epithelium (RPE), parafoveal temporal and nasal retinal thickness (μm) and other qualitative parameters such as the presence of hyporeflective inner retinal cavities, ILM drape sign, disruption of EZ and outward bending of inner retinal layers. The retinal thicknesses (from ILM to RPE) in the central and parafoveal areas as defined in the early treatment diabetic retinopathy study chart (The central 1 mm and parafoveal 1–3 mm ring) were measured and recorded with the automated macular cube scanning mode.

The 6 × 6 mm OCTA scans were done in all patients. The vessel densities (VDs) were evaluated by the software available in the OCTA. The superficial capillary plexus (SCP) was defined as the area from 3 μm below the ILM to 15 μm below the inner plexiform layer, and the deep capillary plexus (DCP) was defined as the area from 15 μm to 70 μm below the inner plexiform layer. The VD values in both the SCP and the DCP, which were calculated automatically by the device based on the parafoveal regions of the early treatment of the diabetic retinopathy study grid, were recorded. The "Auto All" function, OCTA position, and image quality of the device were determined and the cases with quality below 7/10 were excluded from the study. Temporal and nasal parafoveal thicknesses were automatically calculated by OCTA. The presence of EZ disruption was graded by reviewing en face OCT slabs for hypo-reflective areas and confirming their status on cross-sectional views.

The macular ganglion cell inner plexiform layer (GCIPL) thickness and the macular retinal nerve fiber layer (RNFL) thickness were measured with OCT (Carl Zeiss, Tokyo, Japan). 512 × 128 macular cube ganglion cell analysis (GCA) algorithm identifies the outer border of RNFL and outer border of IPL and automatically measures the macular GCIPL thickness. Figure 2 shows the measurement of the average and minimum GCIPL and RNFL thicknesses delivered by the device. We performed the GCA algorithm for each patient.

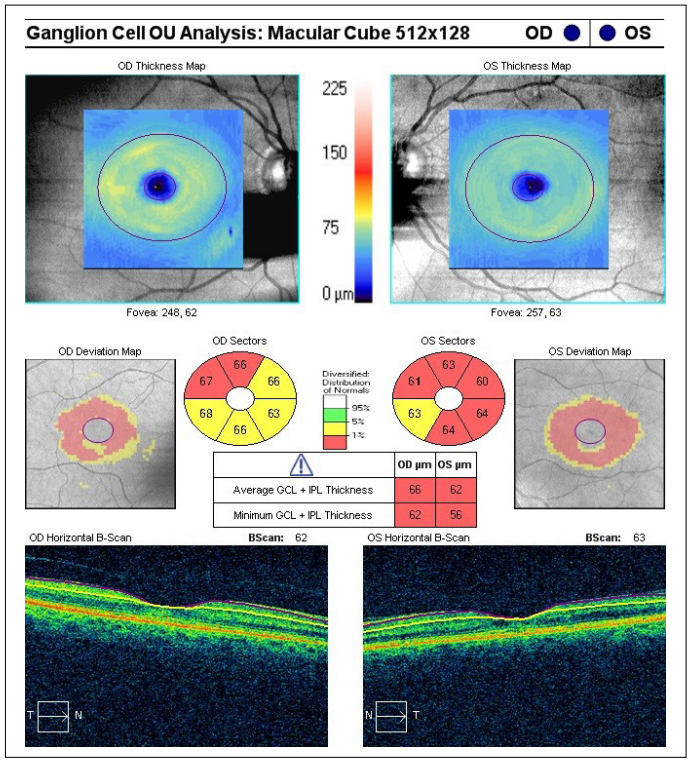

Fig. 2. Macular ganglion cell inner plexiform layer (GCIPL) report shows the average, minimum GCIPL and retinal nerve fiber layer thicknesses and GCIPL segmentation on B scan.

Statistical Analysis

The SPSS 21.0 (SPSS, Inc., Chicago, IL) software was performed for statistical calculations. Constant variables were presented as mean±SD, whereas qualitative variables were given as frequencies and percentages (%). Normality was checked with Shapiro–Wilk, and p>0.05 was considered normal. The contingency tables and Chi-square test or Fisher's test (when required) were done to compare the categorical variables. A paired Student t-test was performed to measure differences between the baseline and 1st-year values among the affected eyes. The one-way analysis of variance with post hoc Bonferroni correction was used to compare the quantitative OCT and OCTA values between the categories. The correlation between the final BCVA and the OCT, OCTA parameters was analyzed by Pearson's correlation. A p<0.05 was considered statistically significant.

Results

The 36 eyes with MacTel Type 2 and 30 eyes as a control group were included in this study. There is no statistically significant difference in terms of age and sex between MacTel and the control group. (For age p=0.802 and for sex p=0.589).

Table 1 shows the comparisons in the baseline clinical characteristics and OCT imaging features of MacTel Type 2 patients and the control group. Ten eyes belonged to Group 1 (MacTel Type 2 patients with intact EZ), the remaining 26 eyes were enrolled in Group 2 (MacTel Type 2 patients with disrupted EZ). Decreased vision was observed in Group 2 (0.51±0.17 logMAR) in comparison to Group 1 (0.32±0.12 logMAR) and control group (0.14±0.08 logMAR) (Table 1). CMT was lesser in Group 2 compared with control group. (Post hocs Group1 vs. Group 2 p=0.764; for Group 1 vs.

Table 1. Baseline clinical characteristics of MacTel type 2 patients and control group

	Group1 n=10	Group 2 n=26	Control n=30	p
BCVA, logMAR	0.32±0.12	0.51±0.17	0.14±0.08	<0.001A
CMT, µm	240.6±22	232.2±35	259.1±38.2	0.026A
Hyporeflective inner retinal cavities, n (%)	8 (80)	23 (88.4)	-	0.672B
ILM drape, n (%)	7 (70)	22 (84.6)	-	0.622B
Outward bending of inner retinal layers, n (%)	8 (80)	22 (84.6)	-	0.242B
Retinal pigment clumps, n (%)	2 (20)	23 (88.6)	-	<0.001B
Right angle vessel, n (%)	6 (60)	20 (76.9)	-	0.163B

BCVA: Best-corrected visual acuity, CMT: Central macular thickness, ILM: Internal limiting membrane, MacTel: Macular telangiectasia, Group 1: MacTel type 2 eyes with intact ellipsoid zone, Group 2: MacTel type 2 eyes with ellipsoid zone disruption. PA: One-way analysis of variance with post hoc Bonferroni correction, PB: Fisher's test

control p=0.235; for Group 2 vs. control p=0.025) There presence of retinal pigment clumps was higher in Group 2 (Table 1).

Table 2 summarizes the OCT and OCTA characteristics in groups at specific time points throughout the follow-up period. A significant decrease was obtained in parafoveal VD in DCP and temporal parafoveal thickness in the 1st year in both groups. The average and minimum GCIPL decreased in Group 2 through to follow-up period. (For average GCIPL p=0.005, for min GCIPL p=0.003) (Table 2). A sample comparison of VDs in superficial and deep capillary plexus through to follow-up time in a MacTel Type 2 eye with EZ disruption was shown in Figure 3.

The comparison of the OCT and OCTA values between groups at 1-year follow-up in MacTel eyes is shown in Table 3. The VD in SCP, temporal and nasal thicknesses, average, and minimum GCIPL were lower in Group 2 compared to Group 1; though there were no statistically significant differences (Table 3). The VD in DCP was lower in Group 2 than in Group 1 (p=0.049). Mean VD in DCP, temporal and nasal thickness, average minimum GCIPL, and RNFL were significantly lower in Group 2 than in control eyes (Table 3).

We obtained a mild-to-moderate negative correlation between the BCVA and the VD in DCP, temporal parafoveal thickness, average, and minimum GCIPL (Table 4).

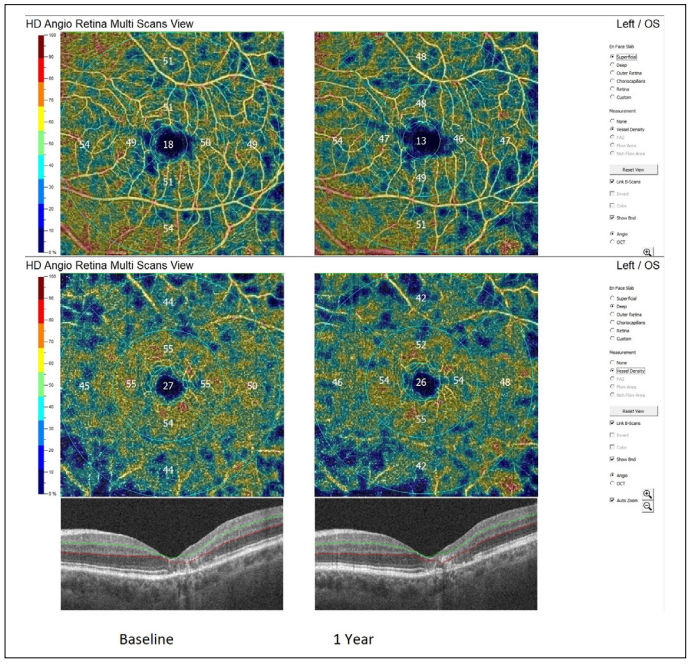

Fig. 3. Comparison of vessel densities in superficial and deep capillary plexus through to follow-up time in a macular telangiectasia type 2 eye with ellipsoid zone disruption.

Table 2. OCT and OCTA characteristics in MacTel eyes and control eyes at specific time-point throughout the follow-up period

	BCVA (logMAR)	Mean±SD								Min RNFL (µm)
		VD in SCP (%)	VD in DCP (%)	FAZ (mm^2)	Temporal RT (µm)	Nasal RT (µm)	Average GCIPL (µm)	Min GCIPL (µm)	Average RNFL (µm)	
Baseline										
Group 1 n=10	0.32±0.12	51.5±2.3	56.5±3.1	0.292±0.07	293.1±14.4	329.9±13.1	77.8±5.1	68.9±7.1	24.3±2.2	11.3±1.7
Group 2 n=26	0.51±0.17	50.6±3.8	54.3±2.5	0.305±0.09	291.3±11.2	327.3±15.6	77.4±4.9	68.6±6.9	25.5±2.3	10.4±1.4
Control n=30	0.14±0.08	52.2±2.4	58.0±4.5	0.257±0.06	322.1±21.9	341.1±13.1	83.8±2.8	72.5±5.8	28.8±1.9	12.4±1.6
1 Year										
Group 1 n=10	0.37±0.11	51.0±2.2	55.4±4.8	0.210±0.04	291.3±14.7	328.4±13.9	77.0±4.1	68.2±7.6	24.5±1.9	11±1.6
Group 2 n=26	0.53±0.13	49.1±3.5	52.3±3.6	0.315±0.05	288.3±10.7	326.6±15.3	74.9±4.4	65.4±6.4	25.2±2.2	10.4±1.3
Control n=30	0.14±0.07	51.6±3.1	58.2±4.2	0.262±0.04	321.6±22.1	341.3±13.9	83.3±3.1	72.1±4.8	28.7±2.1	12.4±1.7
p^A	0.786	0.652	0.006	0.882	0.045	0.083	0.526	0.127	0.336	0.174
p^B	0.689	0.103	0.002	0.343	0.02	0.192	0.005	0.003	0.186	0.330
p^C	0.892	0.183	0.398	0.687	0.142	0.264	0.205	0.467	0.557	0.662

Group 1: MacTel type 2 eyes with intact ellipsoid zone, Group 2: MacTel type 2 eyes with ellipsoid zone disruption. VD: Vessel density, SCP: Superficial capillary plexus, DCP: Deep capillary plexus, GCIPL: Ganglion cell inner plexiform layer complex, RT: Retinal thickness at parafoveal area, SD: standard deviation, MacTel: Macular telangiectasia, OCT: Optical coherence tomography, OCTA: Optical coherence tomography angiography, BCVA: Best-corrected visual acuity. PA: (For Group 1; Baseline vs. 1 year), PB: (For Group 2, Baseline vs. 1 year), and PC: (For Control group, Baseline vs. 1 year).

Table 3. Comparison of the OCT and OCTA features between groups at 1 year in eyes with MacTel type 2

	Group 1 n=10	Group 2 n=26	Control n=30	P^A	P^B	P^C
VD in SCP, (%)	51.4±2.2	49.7±3.5	51.6±3.1	0.188	0.885	0.132
VD in DCP, (%)	55.4±4.8	52.3±3.6	58.2±4.2	0.049	0.085	<0.001
FAZ, mm^2	0.210±0.04	0.315±0.05	0.262±0.04	0.281	0.115	0.911
Temporal parafoveal thickness, µm	291.3±14.7	288.3±10.7	321.6±22.1	0.875	<0.001	<0.001
Nasal parafoveal thickness, µm	328.4±13.9	326.6±15.3	341.3±13.9	0.927	0. 016	0.002
Average GCIPL thickness, µm	77.0±4.1	74.9±4.4	83.3±3.1	0.230	<0.001	<0.001
Min GCIPL thickness, µm	68.2±7.6	65.4±6.4	72.1±4.8	0.390	0.126	0.001
Average RNFL thickness, µm	24.5±1.9	25.2±2.2	28.7±2.1	0.607	<0.001	<0.001
Min RNFL thickness, µm	11±1.6	10.4±1.3	12.4±1.7	0.501	0.014	<0.001

VD: Vessel density, SCP: Superficial capillary plexus, DCP: Deep capillary plexus, GCIPL: Ganglion cell inner plexiform layer complex, RT; Retinal thickness at parafoveal area, SD: standard deviation, MacTel: Macular telangiectasia, OCT: Optical coherence tomography, OCTA: Optical coherence tomography angiography, RNFL: Retinal nerve fiber layer, post hocs. PA: Group 1 versus Group 2, PB: Group 1 versus control, PC: Group 2 versus control.

Table 4. Correlation between BCVA and OCTA-OCT parameters in patients with MacTel Type 2 at 1 year

	BCVA (logMAR)	
	P	r
VD in SCP, (%)	0.062	−0.213
VD in DCP, (%)	<0.001	−0.453
FAZ, mm^2	0.103	0.201
Temporal parafoveal thickness, µm	<0.001	−0.457
Nasal parafoveal thickness, µm	0.06	−0.179
Average GCIPL thickness, µm	0.001	−0.447
Min GCIPL thickness, µm	0.001	−0.513
Average RNFL thickness, µm	0.204	−0.251
Min RNFL thickness, µm	0.071	−0.318

r: Pearson's correlation coefficient. VD: Vessel density, SCP: Superficial capillary plexus, DCP: Deep capillary plexus, FAZ: Foveal avascular zone. Bold values are statistically significant. MacTel: Macular telangiectasia, OCT: Optical coherence tomography, OCTA: Optical coherence tomography angiography, BCVA: Best-corrected visual acuity, RNFL: Retinal nerve fiber layer, GCIPL: Ganglion cell inner plexiform layer complex.

Discussion

In the current study, significant decrements were observed in parafoveal VD in DCP and temporal parafoveal thickness in the 1st year in all MacTel eyes. In addition, GCIPL complex thickness was significantly decreased in MacTel eyes with EZ disruption through to follow-up period.

Although the pathophysiology remains unclear, previous studies suggest that the disease is associated with Muller cell destruction and consequent loss of photoreceptors in the juxtafoveal region.[4,10] Disruption of photoreceptors is seen with disruption of the EZ. Although some cones survived in that area, a tremendous loss of rods was seen.[11] There is also another study showing that the disruption of the interdigitation zone is associated with a reduction in cone number, even if the EZ is intact.[12] Furthermore, it was shown that photoreceptor loss or degeneration leads to new vessels on the outer retina.[13,14] Shen et al., reported that the selective ablation of Muller cells causes cone and rod apoptosis and neovascularization in the outer retina in their animal experiments.[15] It is known that the neovascularization of MacTel Type 2 is likely secondary to photoreceptor loss as a result of Muller cell dysfunction or death. The disruption of EZ was suggested to be preserved as a finding of disease severity and progression. Previous studies supported that the EZ loss is correlated with the decrease in photoreceptor cell density and it is associated with reduced retinal sensitivity.[10,16-19]

Runkle et al. suggested that the reduction in EZ-RPE thickness compared to control eyes may provide a quantitative measure for evaluating the progression and severity of the MacTel Type 2 disease.[8] They also found that the mean central EZ-RPE thickness was significantly correlated with BCVA. Pauleikhoff et al. reported that in OCT, the severity of disease is qualified by progressive EZ damage, which may be assessed as a practical clinical term "disease severity ranking." They also showed that the progression of MacTel correlated remarkably with structural microvascular changes (the number of branches and vessel segments) such as fractal dimension.[20] In our study, we divided our non-proliferative MacTel Type 2 cases into two groups according to the presence of EZ disruption. We compared these two groups according to anatomical features and visual acuity over time. The cases with disrupted EZ had poorer vision and lower VDs and retinal thickness in our study. We speculated that EZ disruption may show disease severity similar to previous

studies and the eyes with EZ disruption may progress more rapidly.

While typical vessel alterations in OCT and FFA may help diagnose, OCT-A allows for differentiation, allocation, and quantifying microvascular alterations within different retinal layers and the choroid.[21] The use of OCT-A in MacTel patients has demonstrated that quantitative values of OCT-A, allow the objective description of vascular patterns and parameters, and differentiate between healthy and damaged microvascular patterns in retinal capillary networks. The microvascular changes in MacTel Type 2 disease were first investigated by Thorell et al., with the OCTA.[22] Spaide et al. showed a decrease of capillary density in the DCP with more prominent qualitative structural changes in MacTel Type 2 patients in their study. These structural changes are defined as capillary dilations, telangiectasis, and the new vessels which are invade the outer retina and subretina in severe cases.[9,22] Observing abnormal retinal capillaries in the normally avascular outer retinal layer and macular neovascular membrane development in OCTA is crucial to choosing the possible treatment for MacTel 2 disease. Venkatesh et al. divided the MacTel eyes based on angiographic perifoveal fluorescence, and OCT features and evaluated the clinical and OCTA features.[23] They concluded in their study that there may be a distinct disease stage called "pre-proliferative" MacTel Type 2 showing clinical features of the non-proliferative disease, difuse + focal perifoveal hyperfluorescent on FFA, absent subretinal neovascularization on OCT, and bunching perifoveal capillaries in DCP on OCTA.[23] Classifying non-proliferative Mactels as such is important for progression management and planning a follow-up visit.

Previous studies reported a decrease in VD in both SCP and DCP eyes with MacTel Type 2.[20,24] Toto et al. compared the MacTel 2 eyes to normal aged-matched controls, their study showed that OCTA parameters had correlations with OCT, early FFA, and late FFA. They observed that the foveal VDs in SCP and DCP and parafoveal retinal thickness were significantly lower in MacTel eyes.[25] The authors demonstrated that OCTA is as valuable and correlated as FFA, the gold standard imaging technique, in the diagnosis of MacTel. A strong correlation was also found with OCT for establishing progressive neurodegenerative changes in MacTel in their study. Similar to previous studies, we also found that as the severity of the disease increased (in the group with EZ disruption), the VDs were lower. In addition, we noticed that mean VD decreased over time in the same group.

RNFL with ganglion cell axons, ganglion cell body (ganglion cell layer), and inner plexiform layer with cell dendrites, these three layers form the retinal ganglion cell complex. Damage to retinal ganglion cells (RGCs) first results in progressive shrinkage of dendritic cells, continued by damage of axons and nucleuses.[26] Thus, as ganglion cells are damaged, the GCIPL complex thickness becomes thinner. OCT technologies and software are very developed and as a result of these imaging techniques, it is probable to estimate the GCIPL complex thickness in vivo and also to quantitatively observe the damage of RGC.[27] The measurement of GCIPL thickness and recognition of ganglion cell loss in vivo are very important, in differential diagnosis of diseases such as glaucoma and optic neuropathic diseases.[28,29] There is also evidence of RGC degeneration in animal models of light-induced retinal degeneration.[30] The cause of ganglion cell damage in retinal pathologies is still unknown. It has been suggested that it may be due to photoreceptor loss or transneuronal degeneration.[31] In MacTel Type 2 disease, the photoreceptor injury occurs later in the course of the disease, while the first damage involves Muller cells affecting the neurosensory retina. Powner et al. found that macular pigment deficit corresponded the decrement of Muller cells as a result of their histological study of the postmortem eye. In addition, the authors found a correlation between loss of EZ and reduction in rod density. They hypothesized that macular pigment depletion usually precedes the disappearance of EZ in MacTel Type 2. If we could measure the macular pigment density in our study, we could obtain data that make our results stronger.[11]

There are no histopathological studies indicating that retina ganglion cells are damaged in MacTel type 2 disease, but in vivo studies show that the GCIPL complex decreases compared to normal eyes in MacTel eyes. The GCIPL thinning continuously in the whole macula and particularly and firstly in the temporal sector suggests ganglion cell damage.[32,33] Chhablani et al. supported that the GCIPL thickness of MacTel eyes was thinner than controls and they speculated that the primary degeneration involves Muller cells, and RGCs degeneration is secondary to Muller cell loss. Furthermore, they also found that RNFL is consistently thinned compared with age-matched controls in MacTel eyes.[33] Similar to previous studies, in our current study we also found a significant decrease in GCIPL complex and RNFL thicknesses in MacTel eyes compared to control group. In addition, in our follow-ups, we found a decrease in average and minimum GCIPL thicknesses over time in MacTel eyes with EZ fracture.

Muller cells extending all the layers of the retina with long-footed protrusions provide oxygen and nutritional sources to retinal neurons and vessels. Furthermore, Muller cells also support the regulatory role. All cells (neurons, muller cells, astrocytes, and vessels) form a functional energy unit to generate the energy necessary for vision, and these cells interact with all aspects of the metabolic process, and each cell recreates a crucial role. [34] The functioning of the metabolic unit is essential for the RGCs, so Muller cell loss may lead to structural alterations and degeneration of the neurosensory retina, including RGCs, leading to progressive thinning. Another theory of neuronal injury may be oxygen and substrate destitution during ischemia, and also reperfusion injury. Retinal ischemia-reperfusion promotes the induction of microglial cells, which leads to immediate degeneration of the ganglion cells and retinal nerve fibers. Decrement of GCIPL thickness and damage of RGCs and other inner retinal neurons is seen as a consequence of the degeneration of the inner retina.

The small sample size and single ethnic group were the most limiting parameters of our study. Another limitation is the possibility of segmentation errors in the GCA algorithm as a result of retinal thinning in MacTel eyes. In cases where there were errors in automatic layering, we manually corrected the segmentation errors on the images and excluded those with poor scan quality from the study.

Conclusion

Our current study showed that VD in SCP, DCP, and GCIPL thickness may be beneficial parameters in the follow-up of MacTel Type 2 patients and provide valuable information about prognosis. With current knowledge, MacTel is considered a primary neurodegenerative disorder with the importance of Muller cell degeneration and loss in the disease process, as different from the first vessel theory. Furthermore, our study indicates that the severity of neurodegenerative and microvascular changes forms in parallel. The assessment of the microvascular differences in the SCP and DCP and the measuring GCIPL thickness may become further characteristics for prospective investigations. Such studies will shed light on a new MacTel clinical classification in the future.

Ethics Committee Approval: This current study was accepted by the Local Institutional Ethics Committee by all ethical standards stated in the Declaration of Helsinki. (Approval number: 18/IV, date: August 26, 2021).

Peer-review: Externally peer-reviewed.

Authorship Contributions: Concept: A.K., S.T.K., A.K.; Design: A.K., C.K., S.T.K.; Supervision: A.K., S.T.K., A.K., S.S.; Resource: C.K., S.T.K.; Materials: C.K., S.T.K., A.K., S.S.; Data Collection and/or Processing: C.K., S.T.K.; Analysis and/or Interpretation: A.K., C.K., S.T.K., A.K., S.S.; Literature Search: A.K., C.K., S.T.K.; Writing: C.K., S.T.K.; Critical Reviews: A.K., S.T.K., S.S.

Conflict of Interest: None declared.

Use of AI for Writing Assistance: Not declared.

Financial Disclosure: The authors declared that this study received no financial support.

References

1. Gass JD, Oyakawa RT. Idiopathic juxtafoveolar retinal telangiectasis. Arch Ophthalmol 1982;100:769-80.[CrossRef]
2. Gass JD, Blodi BA. Idiopathic juxtafoveolar retinal telangiectasis. Update of classification and follow-up study. Ophthalmology 1993;100:1536-46.[CrossRef]
3. Yannuzzi LA, Bardal AM, Freund KB, Chen KJ, Eandi CM, Blodi B. Idiopathic macular telangiectasia. Arch Ophthalmol 2006;124:450-60.[CrossRef]
4. Charbel Issa P, Gillies MC, Chew EY, Bird AC, Heeren TF, Peto T, et al. Macular telangiectasia type 2. Prog Retin Eye Res 2013;34:49-77. [CrossRef]
5. Zeimer MB, Padge B, Heimes B, Pauleikhoff D. Idiopathic macular telangiectasia type 2: Distribution of macular pigment and functional investigations. Retina 2010;30:586-95.[CrossRef]
6. Çoban Karataş M, Yilmaz G, Yüce Sezen A, Saritürk Ç. Clinical features of untreated type 2 macular telangiectasia and efficacy of anti-vascular endothelial growth factor therapy in macular neovascularization. Turk J Ophthalmol 2022;52:45-9. [CrossRef]
7. Heeren TFC, Kitka D, Florea D, Clemons TE, Chew EY, Bird AC, et al. Longitudinal correlation of ellipsoid zone loss and functional loss in macular telangiectasia type 2. Retina 2018;38:S20-6.[CrossRef]
8. Runkle AP, Kaiser PK, Srivastava SK, Schachat AP, Reese JL, Ehlers JP, et al. OCT angiography and ellipsoid zone mapping of macular telangiectasia Type 2 from the AVATAR study. Invest Ophthalmol Vis Sci 2017;58:3683-9.[CrossRef]
9. Spaide RF, Klancnik JM Jr., Cooney MJ. Retinal vascular layers imaged by fluorescein angiography and optical coherence tomography angiography. JAMA Ophthalmol 2015;133:45-50. [CrossRef]
10. Gaudric A, Krivosic V, Tadayoni R. Outer retina capillary invasion and ellipsoid zone loss in macular telangiectasia type 2 imaged by optical coherence tomography angiography. Retina 2015;35:2300-6.[CrossRef]
11. Powner MB, Gillies MC, Zhu M. Loss of Muller's cells and photoreceptors in macular telangiectasia type 2. Ophthalmology 2013;120:2344-52.[CrossRef]
12. Jacob J, Paques M, Krivosic V, Dupas B, Couturier A, Kulcsar C, et al. Meaning of visualizing retinal cone mosaic on adaptive

optics images. Am J Ophthalmol 2015;159:118-23.e1.[CrossRef]
13. Hu W, Jiang A, Liang J, Meng H, Chang B, Gao H, et al. Expression of VLDLR in the retina and evolution of subretinal neovascularization in the knockout mouse model's retinal angiomatous proliferation. Invest Ophthalmol Vis Sci 2008;49:407-15.[CrossRef]
14. Zhao M, Andrieu-Soler C, Kowalczuk L, Paz Cortés M, Berdugo M, Dernigoghossian M, et al. A new CRB1 rat mutation links Muller glial cells to retinal telangiectasia. J Neurosci 2015;35:6093-106.[CrossRef]
15. Shen W, Fruttiger M, Zhu L, Chung SH, Barnett NL, Kirk JK, et al. Conditional mullercell ablation causes independent neuronal and vascular pathologies in a novel transgenic model. J Neurosci 2012;32:15715-27. [CrossRef]
16. Sallo FB, Peto T, Egan C, Wolf-Schnurrbusch UE, Clemons TE, Gillies MC, et al. The IS/OS junction layer in the natural history of type 2 idiopathic macular telangiectasia. Invest Ophthalmol Vis Sci 2012;53:7889-95. [CrossRef]
17. Takayama K, Ooto S, Tamura H, Yamashiro K, Otani A, Tsujikawa A, et al. Retinal structural alterations and macular sensitivity in idiopathic macular telangiectasia type 1. Retina 2012;32:1973-80. [CrossRef]
18. Wolff B, Basdekidou C, Vasseur V, Sahel JA, Gaudric A, Mauget-Faÿsse M. "En face" optical coherence tomography imaging in type 2 idiopathic macular telangiectasia. Retina 2014;34:2072-8. [CrossRef]
19. Maruko I, Iida T, Sekiryu T, Fujiwara T. Early morphological changes and functional abnormalities in group 2A idiopathic juxtafoveolar retinal telangiectasis using spectral domain optical coherence tomography and microperimetry. Br J Ophthalmol 2008;92:1488-91. [CrossRef]
20. Pauleikhoff D, Gunnemann F, Book M, Rothaus K. Progression of vascular changes in macular telangiectasia type 2: Comparison between SD-OCT and OCT angiography. Graefes Arch Clin Exp Ophthalmol 2019;257:1381-92. [CrossRef]
21. Spaide RF, Fujimoto JG, Waheed NK, Sadda SR, Staurenghi G. Optical coherence tomography angiography. Prog Retin Eye Res 2018;64:1-55. [CrossRef]
22. Thorell MR, Zhang Q, Huang Y, An L, Durbin MK, Laron M, et al. Swept-source OCT angiography of macular telangiectasia type 2. Ophthalmic Surg Lasers Imaging Retina 2014;45:369-80. [CrossRef]
23.Venkatesh R, Reddy NG, Mishra P, Pereira A, Mutalik D, Agrawal S, et al. The preproliferative stage in type 2 macular telangiectasia (MacTel type 2). Graefes Arch Clin Exp Ophthalmol 2022;260:121-32. [CrossRef]
24. Chidambara L, Gadde SG, Yadav NK, Jayadev C, Bhanushali D, Appaji AM, et al. Characteristics and quantification of vascular changes in macular telangiectasia type 2 on optical coherence tomography angiography. Br J Ophthalmol 2016;100:1482-8. [CrossRef]
25. Toto L, Di Antonio L, Mastropasqua R, Mattei PA, Carpineto P, Borrelli E, et al. Multimodal imaging of macular telangiectasia type 2: Focus on vascular changes using optical coherence tomography angiography. Invest Ophthalmol Vis Sci 2016;57:OCT268-76. [CrossRef]
26. Leung CK, Weinreb RN, Li ZW, Liu S, Lindsey JD, Choi N, et al. Long-term in vivo imaging and measurement of dendritic shrinkage of retinal ganglion cells. Invest Ophthalmol Vis Sci 2011;52:1539-47. [CrossRef]
27. Tatham AJ, Meira-Freitas D, Weinreb RN, Marvasti AH, Zangwill LM, Medeiros FA. Estimation of retinal ganglion cell loss in glaucomatous eyes with a relative afferent pupillary defect. Invest Ophthalmol Vis Sci 2014;55:513-22. [CrossRef]
28. Sung MS, Yoon JH, Park SW. Diagnostic validity of macular ganglion cell-inner plexiform layer thickness deviation map algorithm using cirrus HD-OCT in preperimetric and early glaucoma. J Glaucoma 2014;23:e144-51. [CrossRef]
29. Gonul S, Koktekir BE, Bakbak B, Gedik S. Comparison of the ganglion cell complex and retinal nerve fibre layer measurements using fourier domain optical coherence tomography to detect ganglion cell loss in non-arteritic anterior ischaemic optic neuropathy. Br J Ophthalmol 2013;97:1045-50. [CrossRef]
30. Garcia-Ayuso D, Salinas-Navarro M, Agudo-Barriuso M, Alarcón-Martínez L, Vidal-Sanz M, Villegas-Pérez MP. Retinal ganglion cell axonal compression by retinal vessels in light-induced retinal degeneration. Mol Vis 2011;17:1716-33.
31. Li ZY, Kljavin IJ, Milam AH. Rod photoreceptor neurite sprouting in retinitis pigmentosa. J Neurosci 1995;15:5429-38. [CrossRef]
32. Narayanan R, Majji AB, Hussain N, Hussain A, Jalali S, Mathai A, et al. Characterization of idiopathic macular telangiectasia type 2 by fundus fluorescein angiography in Indian population. Eur J Ophthalmol 2008;18:587-90.[CrossRef]
33. Chhablani J, Rao HB, Begum VU, Jonnadulla GB, Goud A, Barteselli G. Retinal ganglion cells thinning in eyes with nonproliferative idiopathic macular telangiectasia type 2A. Invest Ophthalmol Vis Sci 2015;56:1416-22.[CrossRef]
34. Yu DY, Cringle SJ, Balaratnasingam C, Morgan WH, Yu PK, Su EN. Retinal ganglion cells: Energetics, compartmentation, axonal transport, cytoskeletons and vulnerability. Prog Retin Eye Res 2013;36:217-46.[CrossRef]